Mechanical behaviour of TWIP steel under shear loading

G. Vincze[1]*, M.C. Butuc[1] and F. Barlat[1,2]

[1]Centre for Mechanical Technology and Automation, University of Aveiro, Campus Universitário de Santiago, 3810-193 Aveiro, Portugal

[2]Graduate Institute of Ferrous Technology, Pohang University of Science and Technology, San 31 Hyoja-dong, Nam-gu, Pohang, Gyeongbuk 790-784, Republic of Korea

gvincze@ua.pt

Abstract. Twinning induced plasticity steels (TWIP) are very good candidate for automotive industry applications because they potentially offer large energy absorption before failure due to their exceptional strain hardening capability and high strength. However, their behaviour is drastically influenced by the loading conditions. In this work, the mechanical behaviour of a TWIP steel sheet sample was investigated at room temperature under monotonic and reverse simple shear loading. It was shown that all the expected features of load reversal such as Bauschinger effect, transient strain hardening with high rate and permanent softening, depend on the prestrain level. This is in agreement with the fact that these effects, which occur during reloading, are related to the rearrangement of the dislocation structure induced during the pre-deformation. The homogeneous anisotropic hardening (HAH) approach proposed by Barlat et al. (2011) [1] was successfully employed to predict the experimental results.

1. Introduction

One of the oldest materials, steel, has been continuously improved over the years, maintaining its supremacy for manufacturing even today. The Twinning Induced Plasticity (TWIP) steel is one of the new steel grades, which exhibit high tensile strength in the range 1300-1500 MPa and significant ductility with strains to failure above 0.3 (30%). This high performance is the result of the exceptional strain hardening ability induced by the TWIP effect [2-4]. The obstacles produced by twins to dislocation glide lead to the reduction of the dislocation mean free path. Recently, it was shown by Bintu et al. [5] that the strain hardening of TWIP steel is strongly dependent on twin density, which can lead to a negative strain hardening rate sensitivity parameter. In the cited work, the author changed the density of twins by varying the strain rate. In the present work, different prestrain amount are considered for the same purpose.

The large flow stress and large ductility of the TWIP steel makes this material useful in applications requiring large energy absorption. Since most applications require that the material deforms plastically under non-proportional loading, the objective of this work is to analyse the mechanical response of TWIP steel subjected to reverse loading when the prestrain is gradually increased. Moreover, this study is conducted to evaluate the capability of the homogeneous anisotropic hardening (HAH) model proposed by Barlat et al [1] to describe the material behaviour.

2. Material and experimental details

An Fe-Mn-C-Si-Al austenitic TWIP steel supplied by POSCO (South Korea) with the chemical composition shown in Table 1 is considered in this study. The material was supplied in the form of sheet of 1.85 mm thickness. The as-received TWIP steel is austenitic at room temperature. The austenite is stabilized by a high concentration of Mn (higher than 15%). Under load, this material twins, but no phase transformation to martensite is observed. Si is added to prevent C precipitation leading to the formation of carbides.

Table 1 Chemical composition of the TWIP steel considered in the present study

C	Mn	Si	Al
0.6%	18%	0.22%	1.5%

The material was tested in simple shear using a Shimadzu Autograph Machine (Shimadzu, Japan) with maximum load capacity of 100 kN and the deformation was measured with ARAMIS - non-contact and material-independent measuring system based on digital image correlation (GOM, Germany). The simple shear device used in this work is an improvement of the previous tool developed at the University of Aveiro. This device compared to others has the particularity that it is compact enough to use it inside a thermic chamber if needed. Fig. 1 shows the simple shear device used in the present work. Moreover, due to the high strength of this material, the geometry of the specimens (Fig. 2) proposed by Guitierez-Urutia et al. [6] is adopted.

Figure 1. Simple shear device for AHSS

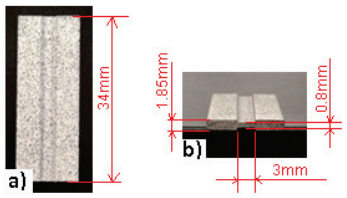

Figure 2. Sample for shear test.
a) front view; b) up view

3. Constitutive Modelling

In this study, an advanced constitutive model based on anisotropic non-quadratic yield functions and a distortional hardening framework, is used. A brief description is given below but more details can be found in [1].

3.1 Swift isotropic hardening model

The Swift model expresses the isotropic strain hardening component in the form of a the power law

$$\sigma = K(\varepsilon_0 + \bar{\varepsilon})^n \tag{1}$$

where $\bar{\varepsilon}$ is the effective plastic strain, and K, ε_0, n are material parameters.

3.2 YLD2000-2D Yield Function

The Yld2000-2d plane stress yield function introduces plastic anisotropy with two linear transformations on the Cauchy stress tensor. It is expressed in terms of the deviatoric stress components as:

$$\phi = \phi'\left(\tilde{\boldsymbol{S}}'\right) + \phi''\left(\tilde{\boldsymbol{S}}''\right) = 2\bar{\sigma}_Y^a, \tag{2}$$

where ϕ' and ϕ'' are two isotropic functions defined by

$$\phi'\left(\tilde{\boldsymbol{S}}'\right) = \left|\tilde{S}'_1 - \tilde{S}'_2\right|^a, \tag{3}$$

$$\phi''\left(\tilde{\boldsymbol{S}}''\right)=\left|2\tilde{S}_2''+\tilde{S}_1''\right|^a+\left|2\tilde{S}_1''+\tilde{S}_2''\right|^a, \tag{4}$$

while $\tilde{\boldsymbol{S}}'$ and $\tilde{\boldsymbol{S}}''$ are linear transformations of the effective stress tensor ***s***, which is defined as the deviatoric part of the Cauchy stress. Hence,

$$\tilde{\boldsymbol{S}}'=\boldsymbol{C}'\,\boldsymbol{s}, \qquad \tilde{\boldsymbol{S}}''=\boldsymbol{C}''\,\boldsymbol{s}, \tag{5}$$

where $\boldsymbol{C}'$ and $\boldsymbol{C}''$ represent the linear transformations of the effective stress tensor **s** and contain the material anisotropy coefficients.

3.3 Homogeneous anisotropic hardening (HAH)

This formulation is a combination of a conventional yield function (which can be isotropic or anisotropic) and a fluctuating component. It is described by the follows equation:

$$\Phi(\mathbf{s})=\left(\phi_s^q+\phi_f^q\right)^{\frac{1}{q}}=\left[\phi_s^q+f_1^q\left|\hat{\mathbf{h}}^{\mathbf{s}}:\mathbf{s}+\left|\hat{\mathbf{h}}^{\mathbf{s}}:\mathbf{s}\right|\right|^q+f_2^q\left|\hat{\mathbf{h}}^{\mathbf{s}}:\mathbf{s}-\left|\hat{\mathbf{h}}^{\mathbf{s}}:\mathbf{s}\right|\right|^q\right]^{\frac{1}{q}}=\sigma(\bar{\varepsilon}) \tag{6}$$

where **s** is the stress deviator and *q* a constant exponent, $\hat{\mathbf{h}}$ is a normalized tensorial state variable, called the microstructure deviator; f_1 and f_2 are two functions of two state variables g1 and g2; g3 and g4 capture the permanent softening. The coefficients k, k_1 to k_5 control the evolution of the microstructure deviator and state variables g_1 to g_4, respectively(see Table 2).

Table 2. The evolutions of the state variables

$\hat{\mathbf{h}}^{\mathbf{s}}:\mathbf{s}\geq 0$	$\hat{\mathbf{h}}^{\mathbf{s}}:\mathbf{s}<0$
$\frac{dg_1}{d\bar{\varepsilon}}=k_2\left(k_3\frac{\bar{\sigma}_0}{\bar{\sigma}(\bar{\varepsilon})}-g_1\right)$ (7)	$\frac{dg_1}{d\bar{\varepsilon}}=k_1\frac{g_4-g_1}{g_1}$ (11)
$\frac{dg_2}{d\bar{\varepsilon}}=k_1\frac{g_3-g_2}{g_2}$ (8)	$\frac{dg_2}{d\bar{\varepsilon}}=k_2\left(k_3\frac{\bar{\sigma}_0}{\bar{\sigma}(\bar{\varepsilon})}-g_2\right)$ (12)
$\frac{dg_4}{d\bar{\varepsilon}}=k_5\left(k_4-g_4\right)$ (9)	$\frac{dg_3}{d\bar{\varepsilon}}=k_5\left(k_4-g_3\right)$ (13)
$\frac{d\hat{\mathbf{h}}_s}{d\bar{\varepsilon}}=k\left(\hat{\mathbf{s}}-\frac{8}{3}\hat{\mathbf{h}}_s\left(\hat{\mathbf{h}}_s:\hat{\mathbf{s}}\right)\right)$ (10)	$\frac{d\hat{\mathbf{h}}_s}{d\bar{\varepsilon}}=-k\left(-\hat{\mathbf{s}}+\frac{8}{3}\hat{\mathbf{h}}_s\left(\hat{\mathbf{h}}_s:\hat{\mathbf{s}}\right)\right)$ (14)

Table 3. Material constitutive coefficients of TWIP steel used for simulation.

Swift law	*K [MPa]*	ε_0	*n*						
	2398	0.12	0.685						
Yld2000-2d	*a*	α_1	α_2	α_3	α_4	α_5	α_6	α_7	α_8
	6	0.9441	1.0407	1.0123	0.9820	1.0322	1.0656	1.0127	0.9965
HAH	*q*	*k*	k_1	k_2	k_3	k_4	k_5		
	2	30	40	45	0.1	0.75	8		

4. Results and discussion

The experimental stress-strain curves of TWIP steel deformed in forward-reverse simple shear loading are shown in Fig. 3. For reverse loading, the amount of prestrain was gradually increased in order to vary the twin density. Besides of a strong Bauschinger effect and a transient hardening stage, it can be observed that the hardening rate decreases with increasing the prestrain amount.

In Fig. 4, the calculated and experimental shear stress-shear strain curves are presented in two graphs for the sake of clarity (two curves in each graph). For low amounts of prestrain, the model captures all the characteristics of the material behaviour very well. On the other hand, for a prestrain of 65%, the

model tends to overestimate the permanent-softening behaviour. One solution is to decrease the coefficient k_4 of HAH model in order to emphasize the permanent softening, but of course this will affect the others curves. Another solution may be the replacement of the Swift model with a hardening law based on the dislocation density.

In conclusion, the HAH model can be used for a reasonably accurate modelling of TWIP steel subjected to reverse loading. In the future, it will be interesting to investigate the behaviour of TWIP steel in cross-loading conditions.

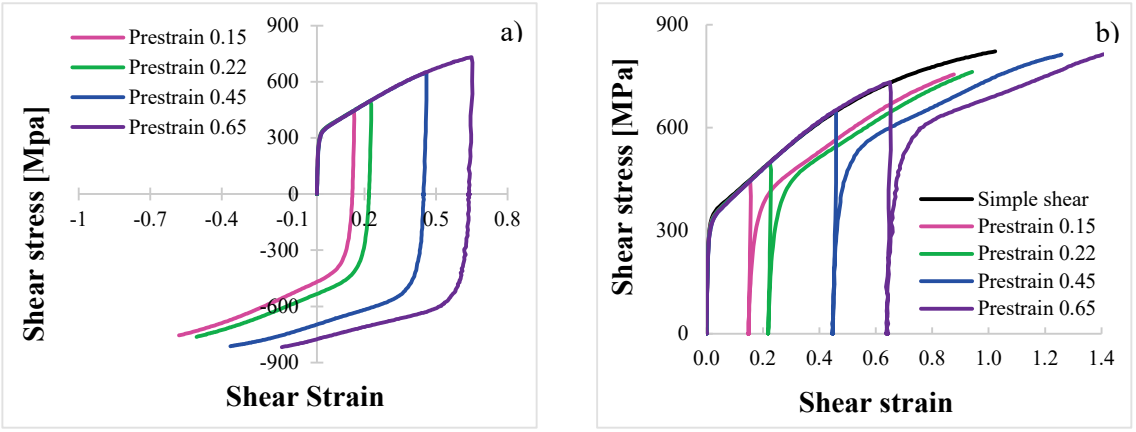

Figure 3. Experimental simple shear stress-strain curves with different prestrain amounts: a) Total strain with absolute stress and; b) cumulated strain and positive stress.

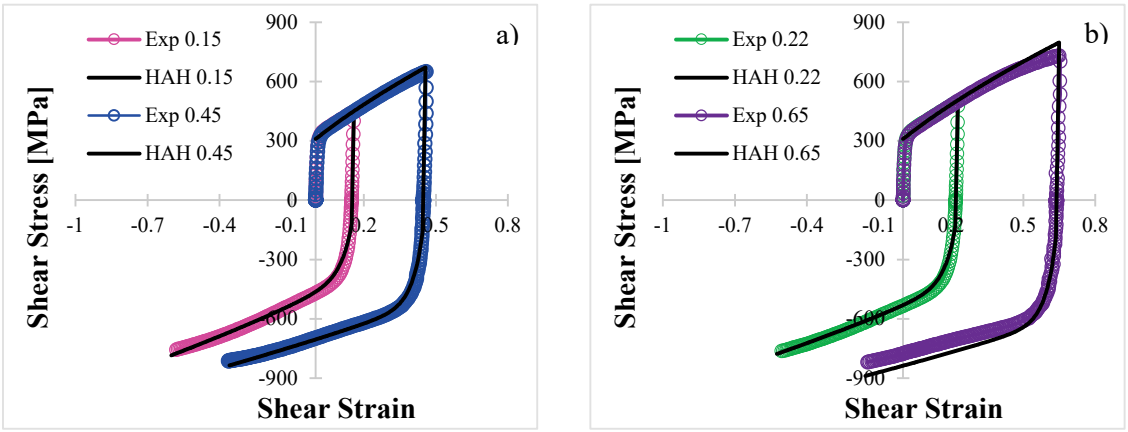

Figure 4. Calculated and experimental results with different prestrain amount: a) 15% and 45% and b) 22% and 65%

Acknowledgments
The authors acknowledge support from the Portuguese Foundation of Science and Technology (FCT) through projects PTDC/EME-PME/116683/2010 and UID/EMS/00481/2013. We thank POSCO (South Korea) for providing the studied material.

References

[1] Barlat F, Gracio J J, Lee M G, Rauch E F and Vincze G, 2011 *Int. J. Plast.* **27** 1309
[2] Barbier D, Gey N, Bozzolo N, Allain S, 2009 Journal of microscopy **235** 67
[3] U.F Kocks, 1996 Phil. Mag. **13** 541
[4] Lebedkina TA, Lebyodkin MA, Chateau JP, Jacques A, Allain S 2009 Mater. Sci. Eng.A **519** 147
[5] A. Bintu, G. Vincze, C. Picu, A. Lopes, J. Grácio, F. Barlat, 2015 Mat. Sci. Eng. A **629** 54
[6] I. Gutierrez-Urrutia, J. A. del Valle, S. Zaefferer, D. Raabe, 2010 *J Mater Sci.* **45** 6604–6610